

# CHEMISTRY

## A **European** Journal

### Supporting Information

#### **A Unified Experimental/Theoretical Description of the Ultrafast Photophysics of Single and Double Thionated Uracils**

Danielle Cristina Teles-Ferreira<sup>+, [a, b]</sup> Irene Conti<sup>+, [c]</sup> Rocío Borrego-Varillas<sup>+, [d]</sup> Artur Nenov<sup>+, [c]</sup>  
Ivo H. M. Van Stokkum,<sup>[e]</sup> Lucia Ganzer,<sup>[d]</sup> Cristian Manzoni,<sup>[d]</sup> Ana Maria de Paula,<sup>\*, [a]</sup>  
Giulio Cerullo,<sup>\*, [d]</sup> and Marco Garavelli<sup>\*, [c]</sup>

chem\_201904541\_sm\_miscellaneous\_information.pdf

# A unified Experimental/Theoretical Description of the Ultrafast Photophysics of Single and Double Thionated Uracils

*Danielle Cristina Teles-Ferreira<sup>‡</sup>, Irene Conti<sup>§</sup>, Rocío Borrego-Varillas<sup>¶</sup>, Artur Nenov<sup>~</sup>, Ivo H. M. Van Stokkum<sup>~</sup>, Lucia Ganzer<sup>†</sup>, Cristian Manzoni<sup>†</sup>, Ana Maria de Paula<sup>¶</sup>, Giulio Cerullo<sup>¶</sup> and Marco Garavelli<sup>¶</sup>*

<sup>‡</sup> Departamento de Física, Universidade Federal de Minas Gerais, 31270-901 Belo Horizonte-MG, Brazil

<sup>¶</sup>Electrical Engineering Department, Federal Institute of Minas Gerais, Formiga - MG, Brazil

<sup>§</sup> Dipartimento di Chimica Industriale, Università degli Studi di Bologna, Viale del Risorgimento 4, I-40136 Bologna, Italy

<sup>†</sup> IFN-CNR, Department of Physics, Politecnico di Milano, P.za L. da Vinci 32, 20133, Milano

<sup>~</sup> Department of Physics and Astronomy, Faculty of Sciences, Vrije Universiteit, De Boelelaan 1081, 1081HV Amsterdam, The Netherlands

## Supporting Information

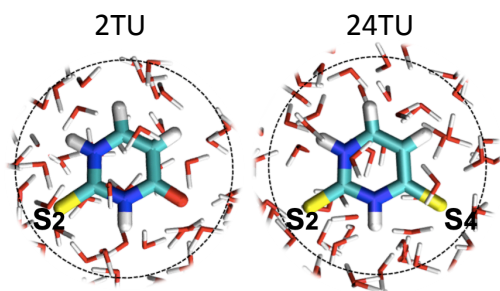
1. Computational details
2. Vertical energies
3. 2TU: Min  $\pi\pi^*(S_2)$ , Min  $n\pi^*(S_2)$  and Min  ${}^3n\pi^*(S_2)$  structures
4. Details on 2TU decay paths and PA/SE signals
5. 24TU: Min  $\pi\pi^*(S_2)$ , Min  $n\pi^*(S_2)$ , Min  ${}^3\pi\pi^*(S_2)$  and Min  ${}^3n\pi^*(S_2)$  structures.
6. Details on 24TU decay paths and PA/SE signals
7. Details on PL measurements
8. Sample preparation
9. Experimental setup
10. Cartesian coordinates of QM part

### 1. Computational details

#### a. Classical molecular dynamics

The 2-thiouracil (2TU) and 2,4-dithiouracil (24TU) starting geometry were obtained running a classical molecular dynamics simulation, using the AMBER 12 suite<sup>[1]</sup> with the ff10 force field. Periodic boundary conditions were applied to a 35 x 34 x 31 Å and 36 x 34 x 31 Å periodic box containing 1229 and 1255 water molecules, described by the TIP3P force field<sup>[2]</sup>. The hydrogen-containing bonds were restrained by the SHAKE algorithm<sup>[3]</sup> while the water geometry was rigidized by the SETTLE scheme<sup>[4]</sup>. Non-bonding and electrostatic interactions were evaluated with a cutoff of 9 Å, making use of the method for quantification of the long-range electrostatics. The time step was set to 0.5 fs and integration of the equations of motion was done with the leap-frog algorithm. Thermalization of the systems was reached by heating of the pre-optimized system to 300 K in 15 ps steps of 100 K. A production run at 300 K and 1 atm was carried out for 500 ps. The lowest energy structure along the dynamics was selected as a starting point for subsequent QM/MM refinement.

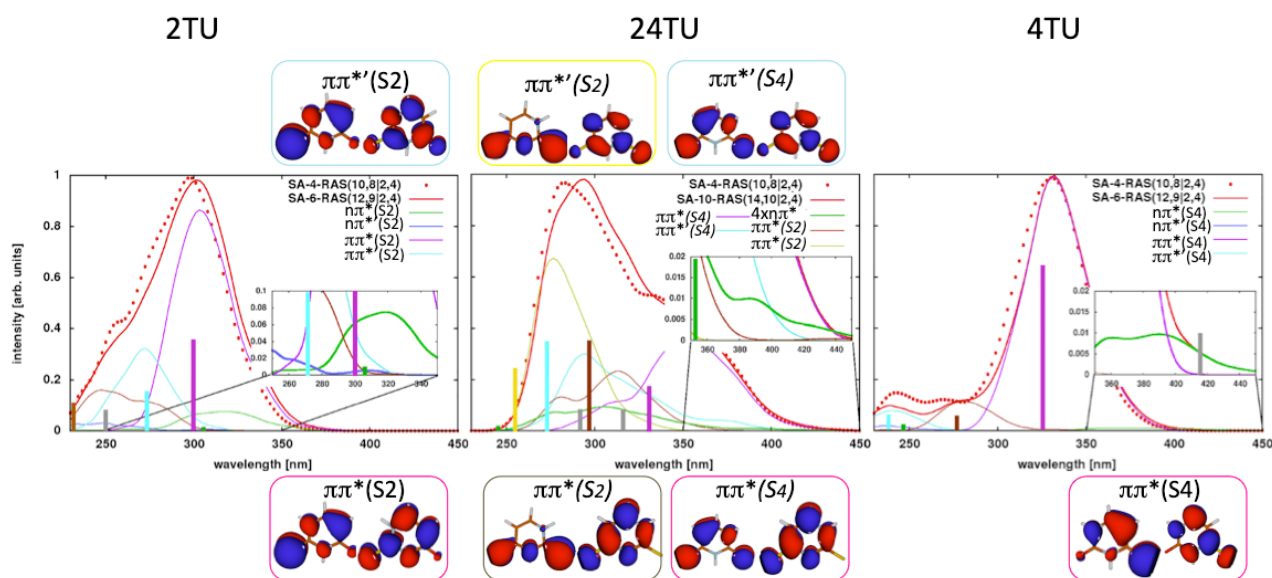
## b. QM/MM layers partitioning.



**Figure S1.** High/Medium/Low layer partitioning of 2TU and 24TU in the QM/MM protocol. The High layer comprises the thionucleobase, the Medium layer comprises all waters in 3 Å distance of the QM region (encircled with a dashed line). The rest of waters are included in the Low layer.

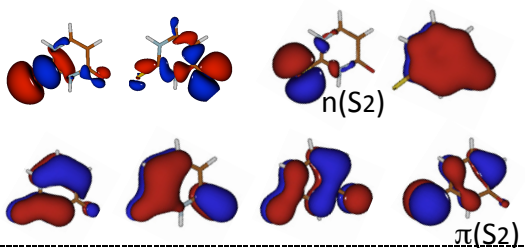
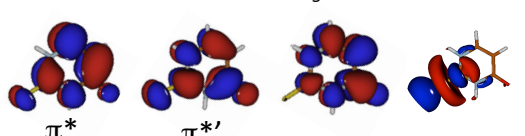
QM/MM calculations were executed with the COBRAMM program, developed in our group interfacing various QM codes with AMBER<sup>[5]</sup>. The High/Medium/Low layers partitioning was applied to a spherical droplet centred at 2TU and 24TU with a radius of 12 Å (containing 261 and 265 waters), obtained from the cubic box. The QM region comprises the thionucleobase. The water molecules in 3 Å distance were included in the movable (MM) Medium layer (Figure S1). The remaining water molecules were kept fixed in the (MM) Low layer.

## 2. Vertical energies

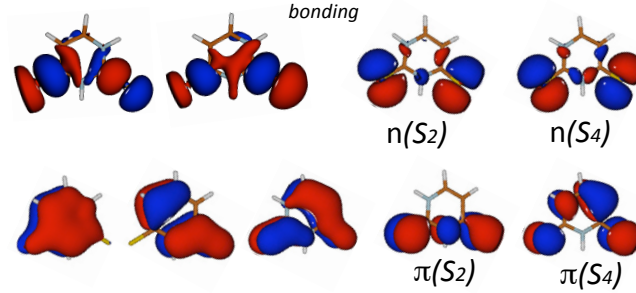
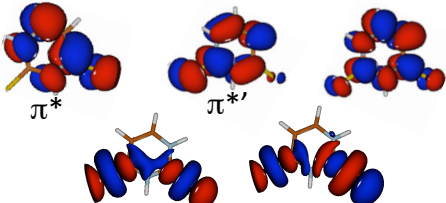


**Figure S2.** Calculated spectra of 2TU, 24TU and 4TU, taken from Chemical Physics 515 (2018) 643–653 publication (MS-RASPT2/SA-6-RASSCF(12,9|2,4)/ANO- $L_S$  level for 2TU and 4TU, MS-RASPT2/SA-9-RASSCF(2,2|14,10|2,2)/ANO- $L_S$  for 24TU). In the present work the decay path of 2TU and 24TU have been mapped at MS-CASPT2/SA-11-CASSCF(16,12)/ANO-RCC and (MS-CASPT2/SA-11-CASSCF(16,12)/ANO-RCC) level, respectively, resembling the order of the states of the present spectra, which employs a larger active space, to better resemble the experimental spectra. Each orbital square represents the Franck-Condon electronic transition involved in the band with the same line colour. The  $\pi$  bonding orbitals of 24TU, in the FC region are still delocalized on both the sulphur atoms; along the relaxation path they localize on S2 or S4, so the respective states  $\pi\pi^*$  or  $\pi\pi^*$  are labelled with ‘(S4)’ or ‘(S2)’, *italics character*<sup>[6]</sup>.

**Table S1.** Vertical excitation energies and oscillator strength ( $f$ ) of 2TU ground state minimum at the MS-RASPT2/SA-6-RASSCF(12,9|2,4)/ANO- $L_5$  (Chemical Physics 515 (2018) 643–653) and at the MS-CASPT2/SA-11-CASSCF(16,12)/ANO-RCC level, both in water.

2TU					
	MS-RASPT2/SA-6-RASSCF(12,9 2,4)/ANO- $L_5$		MS-CASPT2/SA-11-CASSCF(16,12)/ANO-RCC		Exp.
State	Energy (eV)	$f$	Energy (eV)	$f$	
$n\pi^*(S_2)$	4.04	0.01	3.75	0.00	
$\pi\pi^*(S_2)$	4.14	0.36	3.84	0.23	4.28
$\pi\pi'^*(S_2)$	4.54	0.15	4.17	0.20	4.59
$n\pi'^*(S_2)$	4.94	0.00	4.35	0.07	
Active space orbitals (16,12)					
<i>bonding</i>					
					
<i>antibonding</i>					
					

**Table S2.** Vertical excitation energies and oscillator strength ( $f$ ) of 24TU ground state minimum at the MS-RASPT2/SA-9-RASSCF(2,2|14,10|2,2)/ANO- $L_5$  (Chemical Physics 515 (2018) 643–653) and at the MS-CASPT2/SA-11-CASSCF(18,14)/ANO-RCC level, both in water. The ' $S_2$ ' or ' $S_4$ ', *italics* character, indicates that along the relaxation path the  $n$  or the  $\pi$  orbitals are localizing on the corresponding sulphur, instead, in the FC region they are still delocalized on both.

24TU					
	MS-RASPT2/SA-9-RASSCF(2,2 14,10 2,2)/ANO- $L_5$		MS-CASPT2/SA-11-CASSCF(18,14)/ANO-RCC		Exp.
State	Energy (eV)	$f$	Energy (eV)	$f$	
$\pi\pi^*(S_4)$	3.76	0.18	3.33	0.17	3.44
$\pi\pi^*(S_2)$	4.22	0.36	3.74	0.30	
$\pi\pi'^*(S_4)$	4.56	0.36	4.18	0.37	4.51
$\pi\pi'^*(S_2)$	4.85	0.23	4.38	0.14	4.77
$\pi\pi^*(S_4)$	3.51	0.02	3.18	0.00	
$\pi\pi'^*(S_2)$	3.90	0.00	3.56	0.00	
$\pi\pi'^*(S_2)$	4.32	0.00	3.94	0.00	
$\pi\pi'^*(S_4)$	5.08	0.01	4.66	0.02	
Active space orbitals (18,14)					
<i>bonding</i>					
					
<i>Antibonding</i>					
					

### 3. 2TU: Min $\pi\pi^*(S_2)$ , Min $n\pi^*(S_2)$ and Min ${}^3n\pi^*(S_2)$ structures

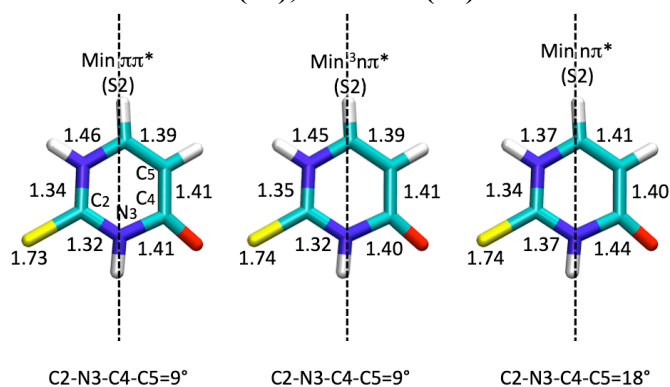


**Figure S3.** Comparison of Min  $\pi\pi^*(S_2)$ , Min  ${}^3n\pi^*(S_2)$  and Min  $n\pi^*(S_2)$  2TU structures. They are similar, and they do not show a large geometrical distortion: the dihedral angle values documented are small, they lead just to a tiny boat distortion of the ring, along the dashed axes.

#### 4. Details on 2TU decay paths and PA/SE signals

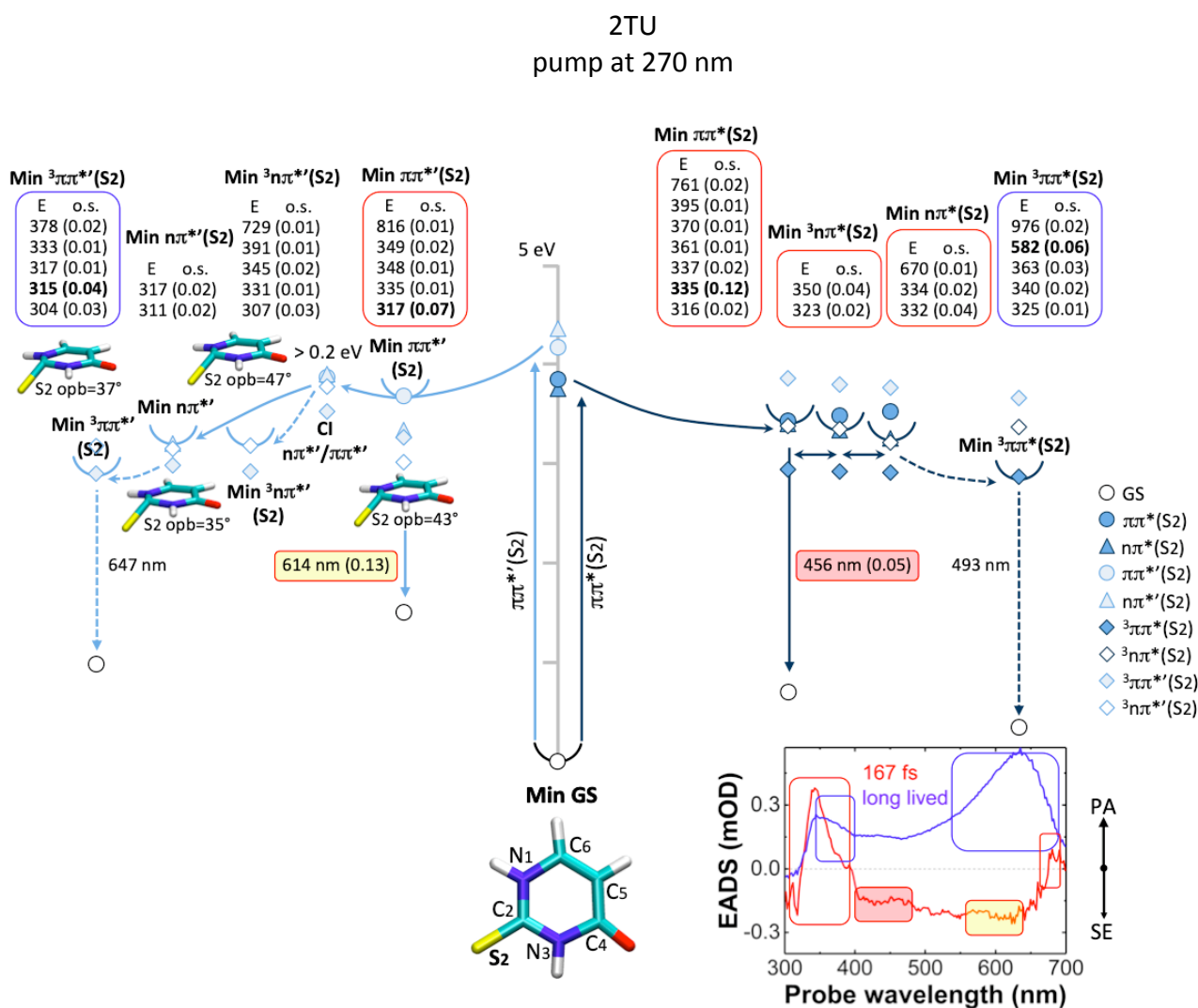


**Figure S4.** This is the more detailed version of Figure 3 in the main text: a larger number of calculated critical points and SE/PA values are documented.

$\pi\pi^*(S_2)$  (on the right) and  $\pi\pi^*(S_2)$  (on the left) decay paths, starting from the Franck-Condon region. The two bright states are excited with the same pumping pulse at  $\lambda=270$ , see Figure 1. The inset EADS panel shows the time constants: the red and blue curves are at 167 fs and long living lifetimes, respectively. Stimulated emission (SE, negative signals) and photoinduced absorption (PA, positive signals) are associated to the calculated SE or PA values evaluated on different minima: they are indicated with red and blue squares if they match with 167 or long living lifetimes signals, respectively.

## 5. 24TU: Min $\pi\pi^*(S_2)$ , Min $n\pi^*(S_2)$ , Min ${}^3\pi\pi^*(S_2)$ and Min ${}^3n\pi^*(S_2)$ structures.

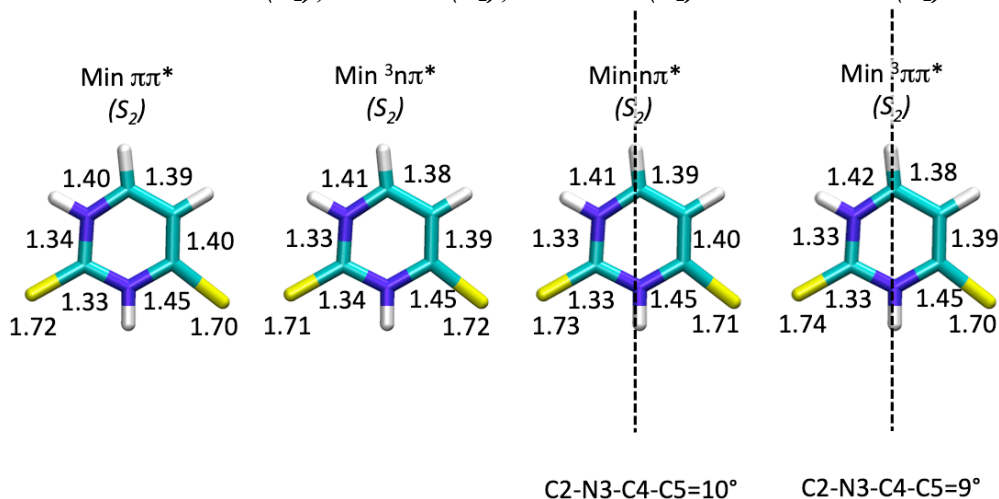


**Figure S5.** Comparison of Min  $\pi\pi^*(S_2)$ , Min  ${}^3n\pi^*(S_2)$ , Min  $n\pi^*(S_2)$  and Min  ${}^3\pi\pi^*(S_2)$  24TU structures. They are similar, and they do not show a large geometrical distortion: the dihedral angle values documented are small, they lead just to a tiny boat distortion of the ring, along the dashed axes.

## 6. Details on 24TU decay paths and PA/SE signals

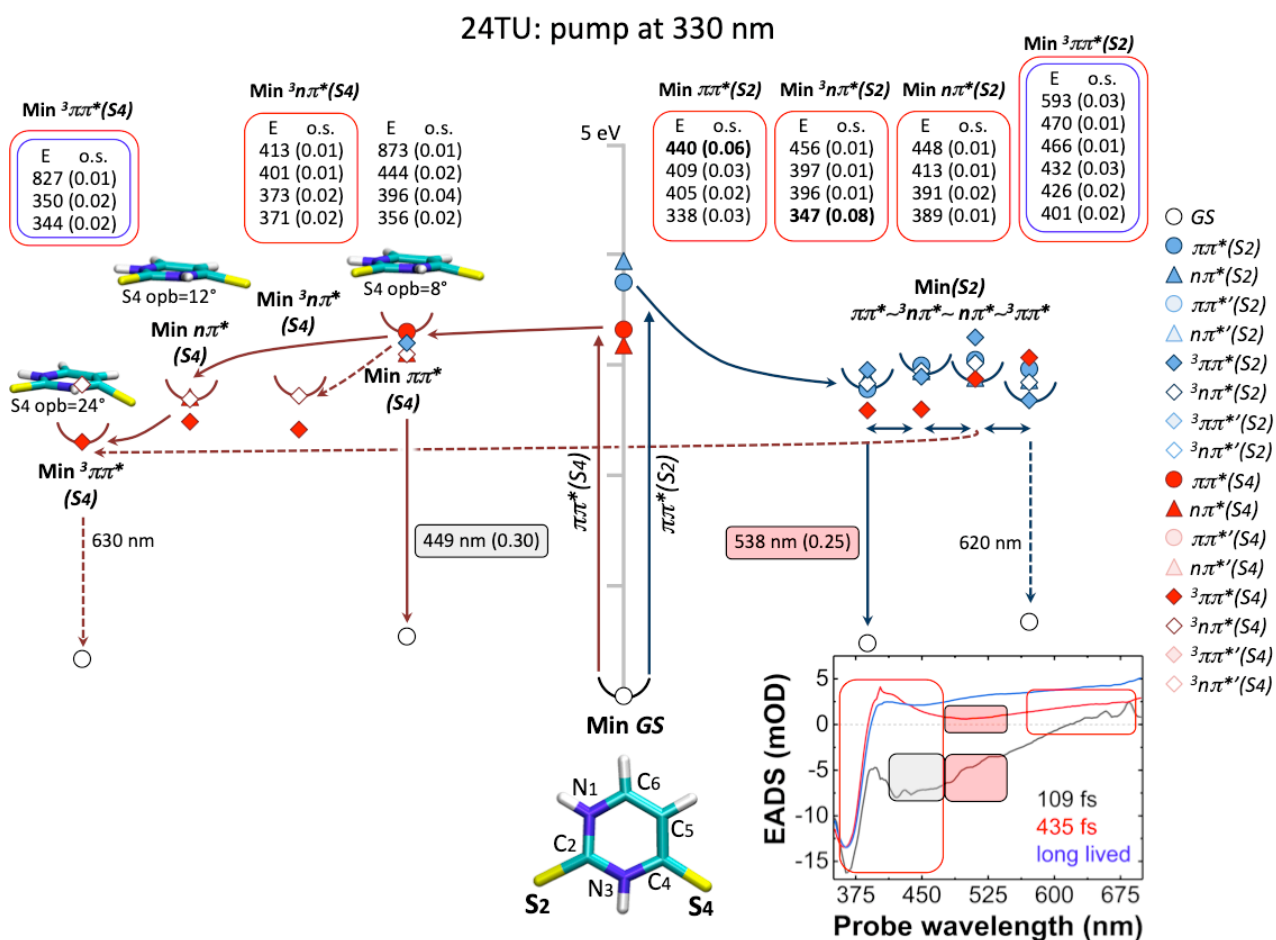


**Figure S6.** This is the more detailed version of Figure 4a in the main text: a larger number of calculated critical point and SE/PA values are documented. Calculated 24TU decay paths pumping with a wavelength of 330 nm.

$\pi\pi^*(S_2)$  (on the right) and  $\pi\pi^*(S_4)$  (on the left). The inset EADS panel shows the time constants: the black, red and blue curves are at 109 fs, 435 and long lived lifetimes, respectively. Stimulated emission (SE, negative signals) and photoinduced absorption (PA, positive signals) are associated to the calculated SE or PA values evaluated on the

different minima: they are indicated with black, red and blue squares if they match with the three different lifetimes signals, 109 fs, 435 fs and long living, respectively.

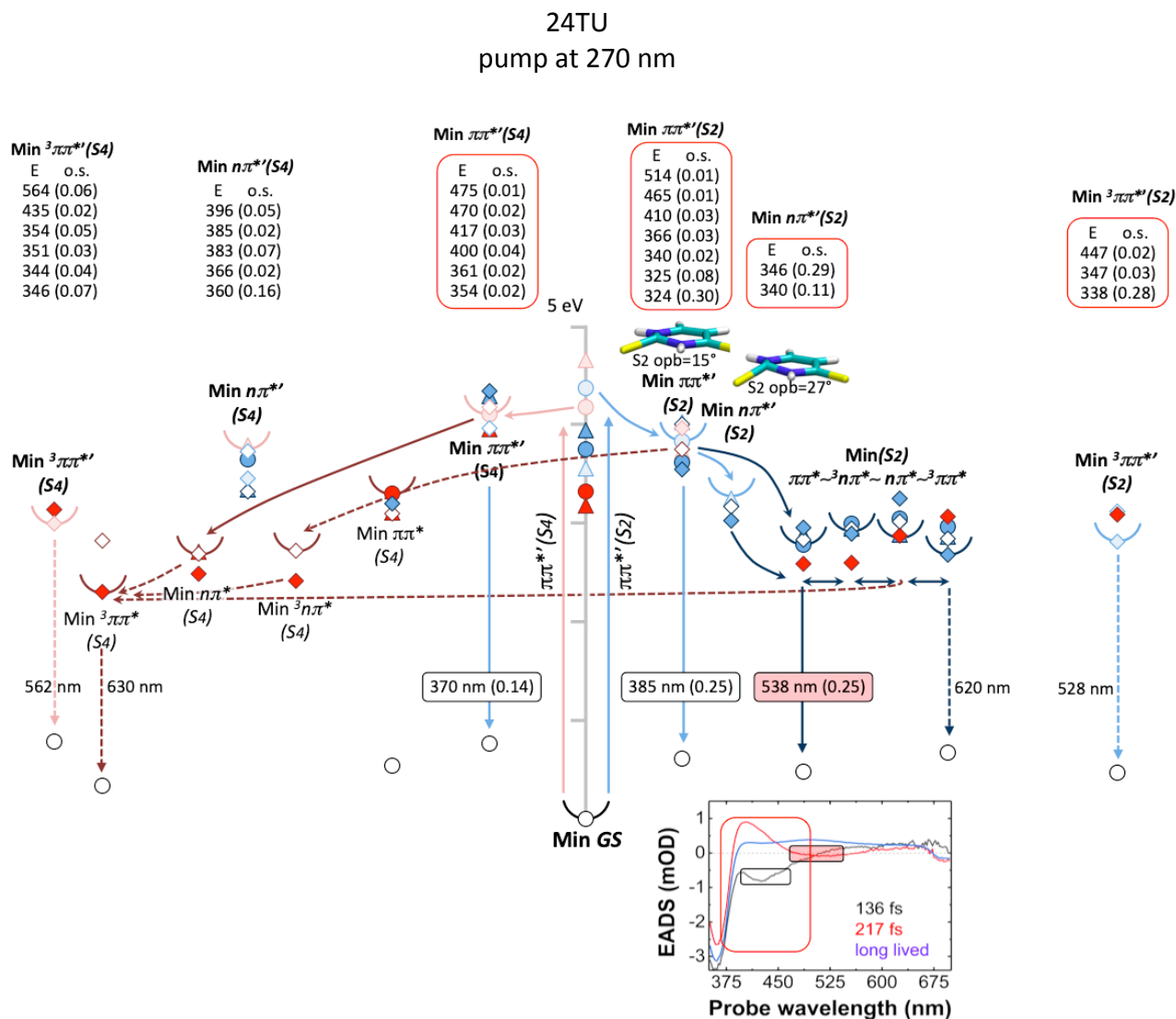


**Figure S7.** This is the more detailed version of Figure 4b in the main text: a larger number of calculated critical point and SE/PA values are documented. Calculated 24TU decay paths pumping with a 270 nm.  $\pi\pi^*(S2)$  (on the right) and  $\pi\pi^*(S4)$  (on the left). The inset EADS panel shows the time constants: the black, red and blue curves are at 136 fs, 217 fs and long living lifetimes, respectively.



## 7. PL measurements

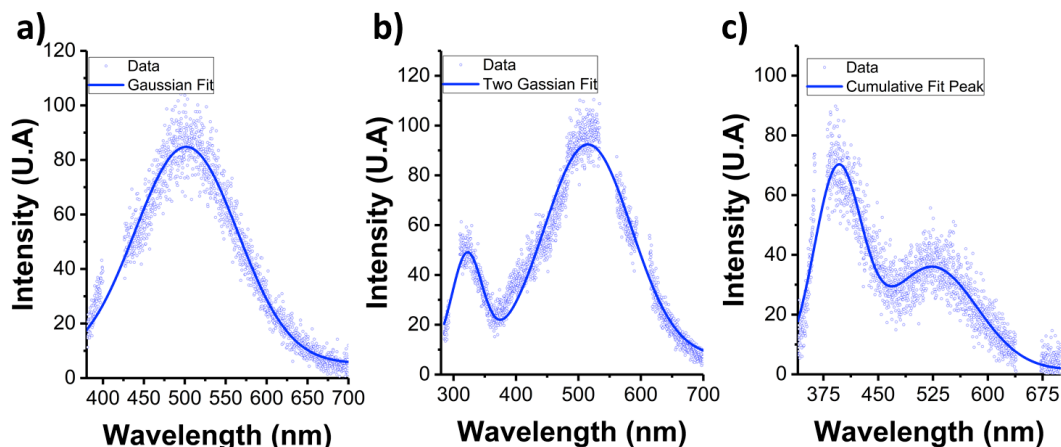


**Figure S8.** Photoluminescence: 2,4-dithiouracil (a) illuminated at 330 nm and (b) illuminated at 270 nm. (c) 4-thiouracil illuminated at 330 nm.

We acquired the steady state emission spectra at room temperature using a Cary Eclipse spectrophotometer, with a white lamp excitation. The spectra were measured at 1000 V PMT voltage with excitation and emission slit-widths of 5 nm and averaging times of 0.9 s. To clear the lamp scattering peaks we performed a background subtraction using the PBS solution. The sample concentrations used were about 0.02 mM.

### a) 2,4-dithiouracil result:

In the 2,4-dithiouracil photoluminescence (PL) excited at 275 nm (Figure S8b) we observe a band from 300 nm to 360 nm (peaking at 320 nm) and another broad band that extends from 360 nm until 700 nm (peaking at 515 nm). The calculations predicted emissions at 370 nm (from  $\pi\pi^*(S_4)$ , Figure S7 on the left), which agrees with the first PL band, and at 538 nm and 385 nm (Figure S7), which agree with the broad PL band around 380-700 nm (Figure S8b). In the pump-probe experiments, we observed a stimulated emission in the short time scale peaking around 400 nm (black line in the EADS, Figure S7 inset) and a stimulated emission peaking around 500 nm (red line in EADS); these results match with the broad PL band. The band from 300 nm to 360 nm was covered by GSB in the pump-probe experiments (Figure 2, in the main text).

In the 2,4-dithiouracil PL excited at 330 nm (Figure S8a) we observe only a broad band that extends from 360 nm until 700 nm (peaking at 500 nm). That is also in agreement with the calculations and the pump-probe experiments. The calculations was predicted emissions at 449 nm and at 538 nm (Figure S6), in agreement with the broad PL band. In the pump-probe experiments, we observed a broad stimulated emission in the short time scale peaking around 420 nm (black line in the EADS, Figure S6 inset) and another broad stimulated emission peaking around 500 nm (red line in EADS); these results also match with the broad PL band results.

### b) 2-thiouracil:

For measurements performed under the same conditions as above, we could not detect PL from the 2-thiouracil.

### c) 4-thiouracil:

Exciting 4-thiouracil at 330 nm, we observed two bands: one band peaking at 400 nm and another band peaking at 520 nm (Figure S8b). These results are in agreement with the literature results,

reported by Taras-Goslinska et al<sup>[7]</sup>. which assigned the first peak as due to a PL from the bright singlet state and the second one as a phosphorescence coming from the triplet state. The result is also in good agreement with the pump-probe experiments, as we observed a stimulated emission at 400 nm and a PA signal about 550 nm due to the triplet state in our previous work<sup>[8]</sup>. And it is also in agreement with the calculations.

## 8. Sample preparation

The PBS solution, 16 mM concentration and 7.4 pH, was prepared by dissolving 0.15 g of sodium dihydrogen phosphate and 0.27 g of sodium hydrogen phosphate in 200 mL of ultrapure water. 4-Thiouracil (97% purity), 2-Thiouracil ( $\geq 99\%$  purity), 2,4-dithiouracil (98% purity) were purchased from Sigma-Aldrich and used as received. 2TU, 4TU and 24TU in PBS solution were prepared to obtain an optical density about 0.5 at the pump wavelength.

## 9. Experimental setup

The experimental TA setup starts with a Ti:Sapphire laser at 800 nm wavelength and 100 fs pulse duration which pumps a non-collinear optical parametric amplifier (NOPA) generating sub-20-fs visible pulses. Our setup allows us to obtain broadband sub-20-fs pump pulses at 330 nm or at 270 nm. Pump pulses at 330 nm are generated by a sum frequency mixing of the NOPA and the fundamental beam. Pump pulses centered at 270 nm come from second harmonic of visible NOPA. Probe pulses (350-600 nm spectral range) are obtained by focusing the fundamental beam on a CaF<sub>2</sub> plate.

## 10. Cartesian coordinates of QM part

### 2TU

	x	y	z
Min GS			
N	18.403175	17.249011	14.500341
C	18.611756	16.345333	15.513430
N	17.621684	16.327185	16.452338
C	16.493385	17.076732	16.358130
C	16.283906	17.914676	15.312981
C	17.267464	18.000455	14.275574
S	19.948326	15.379312	15.565656
O	17.157657	18.685952	13.241638
H	15.362777	18.467249	15.229867
H	15.781902	16.954063	17.161790
H	19.119941	17.240759	13.771186
H	17.701288	15.659531	17.224328

### Min $\pi\pi^*(S_2)$

N	18.399442	17.291251	14.478945
C	18.520594	16.404917	15.470795
N	17.591813	16.324433	16.412669
C	16.445834	17.151397	16.411042
C	16.253372	17.958375	15.273062
C	17.188417	18.072163	14.247801
S	19.906392	15.364873	15.498879
O	17.152399	18.731435	13.163961
H	15.323748	18.497068	15.172575

H	15.746695	16.987966	17.208413
H	19.114320	17.276916	13.749464
H	17.688009	15.622142	17.149593

Min  $n\pi^*(S_2)$

N	18.441484	17.347948	14.503976
C	18.529952	16.372662	15.465688
N	17.593472	16.328611	16.423238
C	16.493003	17.137212	16.407977
C	16.254416	17.942194	15.280530
C	17.206451	18.037083	14.254410
S	19.830849	15.215948	15.382005
O	17.130233	18.661129	13.171119
H	15.317225	18.459797	15.165860
H	15.818548	16.998253	17.233303
H	19.130675	17.355867	13.751192
H	17.642869	15.628925	17.164533

Min  ${}^3\pi\pi^*(S_2)$

N	18.393952	17.287761	14.465225
C	18.558311	16.363975	15.490939
N	17.602025	16.322567	16.444652
C	16.485121	17.079056	16.418888
C	16.266734	17.937356	15.280328
C	17.220109	18.038178	14.240001
S	19.918671	15.357179	15.500151
O	17.165409	18.710845	13.193139
H	15.352111	18.481151	15.197399
H	15.775153	16.946233	17.215035
H	19.115371	17.270049	13.746921
H	17.722451	15.623619	17.197455

Min  ${}^3n\pi^*(S_2)$

N	18.406546	17.273796	14.481253
C	18.535734	16.383846	15.486230
N	17.617505	16.306830	16.438203
C	16.461706	17.097311	16.406501
C	16.271251	17.936569	15.289898
C	17.199757	18.047842	14.260655
S	19.906555	15.318374	15.469870
O	17.165017	18.718144	13.206254
H	15.347016	18.481441	15.203298
H	15.771955	16.953754	17.213735
H	19.102670	17.269206	13.737474
H	17.708022	15.615286	17.190820

Min  $\pi\pi^*(S_2)$

N	18.504996	17.400355	14.587852
C	18.779888	16.635304	15.710033
N	17.685370	16.370014	16.495007
C	16.485968	16.982005	16.327182

C	16.271825	17.828697	15.277517
C	17.305451	18.017155	14.288141
S	19.746916	15.102228	15.287700
O	17.166878	18.664187	13.240856
H	15.310515	18.290064	15.126065
H	15.731481	16.746276	17.061049
H	19.254759	17.445290	13.892049
H	17.779278	15.687680	17.250691

Min  $n\pi^*(S_2)$

N	18.476569	17.367935	14.521832
C	18.682461	16.463077	15.584582
N	17.584935	16.265964	16.409332
C	16.468638	17.019127	16.318710
C	16.290267	17.926552	15.301727
C	17.303117	18.055191	14.288465
S	19.731123	15.063527	15.216351
O	17.191588	18.758225	13.261847
H	15.369271	18.473192	15.198204
H	15.740586	16.854368	17.097676
H	19.186515	17.396683	13.791425
H	17.625369	15.564447	17.147150

Min  ${}^3\pi\pi^*(S_2)$

N	18.505112	17.376105	14.548519
C	18.756717	16.510170	15.636668
N	17.648341	16.275909	16.434745
C	16.500546	16.963990	16.330449
C	16.311799	17.881948	15.316020
C	17.330435	18.043943	14.308173
S	19.753312	15.099340	15.270175
O	17.188913	18.726115	13.275650
H	15.373107	18.394644	15.194283
H	15.756410	16.745322	17.081696
H	19.230763	17.412772	13.830669
H	17.720788	15.576256	17.176447

Min  ${}^3n\pi^*(S_2)$

N	18.529342	17.395975	14.529347
C	18.804614	16.518913	15.596947
N	17.717794	16.307324	16.440396
C	16.537349	16.959871	16.301670
C	16.318256	17.838253	15.279468
C	17.350422	18.041911	14.286123
S	19.620503	14.984888	15.197112
O	17.206811	18.747983	13.270679
H	15.367280	18.327727	15.160018
H	15.795782	16.740907	17.054020
H	19.256111	17.467520	13.818768
H	17.807062	15.652314	17.216238

24TU

Min  $GS$

C	17.758259	16.301956	14.599256
N	18.131411	17.579559	14.275706
C	18.362328	18.552341	15.193150
C	18.263603	18.303587	16.524494
C	17.939247	16.986065	16.971378
N	17.663614	16.092123	15.958480
H	18.477682	19.068405	17.253531
S	17.895147	16.522793	18.563305
S	17.459146	15.141303	13.472569
H	18.646601	19.512947	14.789116
H	17.358847	15.157816	16.223301
H	18.249556	17.797768	13.287046

Min  $\pi\pi^*(S_2)$

C	17.737444	16.395065	14.677117
N	18.148996	17.600023	14.266823
C	18.378202	18.650339	15.170108
C	18.287811	18.357527	16.529253
C	17.934614	17.094496	17.023293
N	17.594048	16.154520	15.978759
H	18.523867	19.127565	17.246267
S	17.883480	16.551371	18.633141
S	17.408489	15.181007	13.506756
H	18.664385	19.592064	14.740294
H	17.234797	15.247050	16.257530
H	18.284239	17.759205	13.268286

Min  $n\pi^*(S_2)$

C	17.773886	16.476948	14.660338
N	18.220205	17.663933	14.255209
C	18.429384	18.713373	15.178601
C	18.360901	18.401293	16.532915
C	17.983831	17.143311	17.019398
N	17.597582	16.232431	15.954591
H	18.610075	19.161192	17.256605
S	17.847700	16.562511	18.621565
S	17.428566	15.244455	13.488943
H	18.721664	19.655771	14.754605
H	17.181494	15.349798	16.239023
H	18.360147	17.833122	13.255933

Min  ${}^3\pi\pi^*(S_2)$

C	17.684340	16.439951	14.702590
N	18.141703	17.610462	14.280084
C	18.397894	18.668219	15.186935
C	18.321251	18.384939	16.539448
C	17.928623	17.144623	17.040173
N	17.518919	16.214836	16.000357

H	18.604784	19.144665	17.251299
S	17.878241	16.577906	18.642086
S	17.300562	15.199031	13.549227
H	18.731140	19.587975	14.745338
H	17.106300	15.338639	16.302065
H	18.315517	17.770645	13.288887

Min  ${}^3n\pi^*(S2)$

C	17.711149	16.404608	14.690280
N	18.148968	17.596910	14.291242
C	18.414450	18.652956	15.193802
C	18.312160	18.378008	16.546486
C	17.918060	17.137650	17.022001
N	17.563747	16.177629	15.999388
H	18.571785	19.144520	17.261412
S	17.848192	16.575315	18.647791
S	17.348783	15.184152	13.547432
H	18.727041	19.581533	14.756976
H	17.196825	15.283829	16.301773
H	18.275585	17.778994	13.294261

Min  $\pi\pi^*(S4)$

C	17.783594	16.342831	14.637950
N	18.146021	17.616531	14.307740
C	18.343447	18.653143	15.158265
C	18.238285	18.378195	16.564533
C	17.899361	17.126265	16.947721
N	17.657263	16.146070	15.991503
H	18.477783	19.135937	17.288795
S	17.861996	16.469725	18.639170
S	17.526588	15.161732	13.499923
H	18.592878	19.605619	14.727089
H	17.315865	15.238995	16.284761
H	18.270391	17.791567	13.309563

Min  $n\pi^*(S4)$

C	17.618736	16.278793	14.589147
N	18.113771	17.509396	14.281196
C	18.372177	18.516499	15.204261
C	18.201616	18.240231	16.544836
C	17.703217	16.997461	16.921392
N	17.389351	16.056097	15.925782
H	18.457745	18.979609	17.289030
S	17.660776	16.459812	18.590361
S	17.331617	15.135631	13.416982
H	18.713480	19.455620	14.806464
H	16.885773	15.201906	16.149252
H	18.269983	17.712898	13.300072

Min  ${}^3\pi\pi^*(S4)$

C	17.598900	16.265930	14.556241
---	-----------	-----------	-----------

N	18.112040	17.510967	14.290597
C	18.350340	18.484674	15.236048
C	18.103756	18.175058	16.571661
C	17.595327	16.927156	16.908131
N	17.348804	16.006716	15.870038
H	18.319799	18.891367	17.348989
S	17.842262	16.331394	18.521654
S	17.342062	15.176579	13.327897
H	18.674236	19.443518	14.872592
H	16.863104	15.130569	16.074253
H	18.289804	17.735119	13.314352

Min  ${}^3n\pi^*(S4)$

C	17.609142	16.267729	14.585656
N	18.127211	17.493641	14.290688
C	18.359919	18.500132	15.218739
C	18.130081	18.228256	16.547295
C	17.593554	16.995544	16.918331
N	17.329517	16.046349	15.911159
H	18.374367	18.954590	17.308334
S	17.654154	16.431200	18.568607
S	17.342627	15.140422	13.390947
H	18.711485	19.439611	14.828950
H	16.804390	15.195272	16.120712
H	18.314299	17.691313	13.311736

Min  $\pi\pi^*(S2)$

C	17.513151	16.444924	14.654642
N	18.078227	17.632854	14.265633
C	18.399327	18.593810	15.171534
C	18.290343	18.345750	16.510933
C	17.928652	17.032499	16.988077
N	17.584823	16.138772	15.993982
H	18.562008	19.097091	17.236183
S	17.924273	16.603844	18.592004
S	17.438371	15.112269	13.404068
H	18.743391	19.531878	14.760475
H	17.215019	15.228979	16.266837
H	18.173578	17.824463	13.266738

Min  $n\pi^*(S2)$

C	17.323312	16.371500	14.859825
N	18.011433	17.528394	14.494918
C	18.407943	18.435730	15.412497
C	18.297637	18.197253	16.755482
C	17.822914	16.921110	17.205342
N	17.408409	16.062492	16.228134
H	18.643829	18.910597	17.482489
S	17.777987	16.471968	18.815272
S	17.479866	14.988486	13.754514
H	18.827524	19.345612	15.013638

H 16.944689 15.214119 16.537695  
H 18.089734 17.779642 13.514799

Min  $\pi\pi^*(S4)$

C	17.633394	16.331984	14.556533
N	18.119053	17.653547	14.258453
C	18.398508	18.580982	15.133155
C	18.269419	18.348942	16.524233
C	17.891102	17.050892	16.881290
N	17.598587	16.134836	15.988890
H	18.514639	19.096144	17.259441
S	17.852577	16.562021	18.613358
S	17.417704	15.106429	13.435891
H	18.733065	19.530424	14.737045
H	17.300552	15.202348	16.265757
H	18.244387	17.863491	13.267159

**References:**

- [1] W. Z. D. A. Case, T. Darden, T. E. Cheatham, C. Simmerling, J. Wang, R. E. Duke, R. Luo, R. C. Walker, *Univ. Calif. San Fr.* **2012**.
- [2] W. L. Jorgensen, J. Chandrasekhar, J. D. Madura, R. W. Impey, M. L. Klein, *J. Chem. Phys.* **1983**, *79*, 926–935.
- [3] J. P. Ryckaert, G. Ciccotti, H. J. C. Berendsen, *J. Comput. Phys.* **1977**, *23*, 327–341.
- [4] S. Miyamoto, P. A. Kollman, *J. Am. Chem. Soc.* **1992**, *114*, 3668–3674.
- [5] P. Altoè, M. Stenta, A. Bottoni, M. Garavelli, *AIP Conf. Proc.* **2007**, *963*, 685–688.
- [6] A. Nenov, I. Conti, R. Borrego-Varillas, G. Cerullo, M. Garavelli, *Chem. Phys.* **2018**, *515*, 643–653.
- [7] K. Taras-Goślińska, G. Wenska, B. Skalski, A. Maciejewski, G. Burdziński, J. Karolczak, *J. Photochem. Photobiol. A Chem.* **2004**, *168*, 227–233.
- [8] R. Borrego-varillas, D. C. Teles-ferreira, A. Nenov, I. Conti, L. Ganzer, C. Manzoni, M. Garavelli, A. M. De Paula, G. Cerullo, *J. Am. Chem. Soc.* **2018**, *140*, 16087–16093.